

ORIGINAL ARTICLE

# $\gamma\delta$ T cells mediate robust anti-HIV functions during antiretroviral therapy regardless of immune checkpoint expression

Kirsty R Field<sup>1</sup> , Kathleen M Wragg<sup>1</sup>, Stephen J Kent<sup>1,2</sup> , Wen Shi Lee<sup>1</sup>  & Jennifer A Juno<sup>1</sup> 

<sup>1</sup>Department of Microbiology and Immunology, University of Melbourne, at the Peter Doherty Institute for Infection and Immunity, Melbourne, VIC, Australia

<sup>2</sup>Melbourne Sexual Health Centre and Department of Infectious Diseases, Central Clinical School, Monash University, Melbourne, VIC, Australia

## Correspondence

JA Juno, University of Melbourne,  
792 Elizabeth St Melbourne, Melbourne,  
VIC 3000, Australia.  
E-mail: [jennifer.juno@unimelb.edu.au](mailto:jennifer.juno@unimelb.edu.au)

Received 3 December 2023;  
Revised 8 January 2024;  
Accepted 13 January 2024

doi: 10.1002/cti2.1486

Clinical & Translational Immunology  
2024; 13: e1486

## Abstract

**Objectives.** Although antiretroviral therapy (ART) efficiently suppresses HIV viral load, immune dysregulation and dysfunction persist in people living with HIV (PLWH).  $\gamma\delta$  T cells are functionally impaired during untreated HIV infection, but the extent to which they are reconstituted upon ART is currently unclear. **Methods.** Utilising a cohort of ART-treated PLWH, we assessed the frequency and phenotype, characterised *in vitro* functional responses and defined the impact of immune checkpoint marker expression on effector functions of both V $\delta$ 1 and V $\delta$ 2 T cells. We additionally explore the *in vitro* expansion of V $\delta$ 2 T cells from PLWH on ART and the mechanisms by which such expanded cells may sense and kill HIV-infected targets. **Results.** A matured NK cell-like phenotype was observed for V $\delta$ 1 T cells among 25 ART-treated individuals (PLWH/ART) studied compared to 17 HIV-uninfected controls, with heightened expression of 2B4, CD160, TIGIT and Tim-3. Despite persistent phenotypic perturbations, V $\delta$ 1 T cells from PLWH/ART exhibited strong CD16-mediated activation and degranulation, which were suppressed upon Tim-3 and TIGIT crosslinking. V $\delta$ 2 T cell degranulation responses to the phosphoantigen (E)-4-hydroxy-3-methyl-but-2-enyl pyrophosphate at concentrations up to 2 ng mL<sup>-1</sup> were significantly impaired in an immune checkpoint-independent manner among ART-treated participants. Nonetheless, expanded V $\delta$ 2 T cells from PLWH/ART retained potent anti-HIV effector functions, with the NKG2D receptor contributing substantially to the elimination of infected cells. **Conclusion.** Our findings highlight that although significant perturbations remain within the  $\gamma\delta$  T cell compartment throughout ART-treated HIV, both subsets retain the capacity for robust anti-HIV effector functions.

**Keywords:** antiretroviral therapy, HIV, immune checkpoint molecules, V $\delta$ 1 T cells, V $\delta$ 2 T cells,  $\gamma\delta$  T cells

## INTRODUCTION

For people living with HIV-1 (PLWH), antiretroviral therapy (ART) efficiently suppresses viral replication and improves immunodeficiency.<sup>1,2</sup> Interruption of treatment results in rapid viral rebound from a reservoir of long-lived provirus-harboring cells.<sup>3,4</sup> The necessity for lifelong adherence to ART holds considerable financial and health-associated effects.<sup>5</sup> In addition, long-term ART does not fully restore immune function, as evidenced by persistent elevated risk of *Mycobacterium tuberculosis* reactivation,<sup>6,7</sup> residual immune activation, exhaustion and dysfunction.<sup>8–12</sup>

One well-described impact of acute HIV-1 (HIV herein) infection is the substantial alteration of the composition and phenotype of unconventional T cells, including  $\gamma\delta$  T cells.  $\gamma\delta$  T cells exhibit MHC-independent reactivity to non-peptide antigens, and in humans are classified into two major subsets by V $\delta$ -chain usage. While the V $\delta$ 1 subset is more frequent at mucosal sites,<sup>13,14</sup> the V $\delta$ 2 subset makes up to 90% of the total  $\gamma\delta$  T cell population within peripheral blood of healthy adults.<sup>15</sup> The most prominent effect of untreated HIV infection on  $\gamma\delta$  T cells is the inversion of typical V $\delta$ 1:V $\delta$ 2 T cell ratios, attributed to the depletion of the V $\gamma$ 9V $\delta$ 2 subset and the concurrent expansion of V $\delta$ 1 T cells<sup>16–19</sup> potentially driven by human cytomegalovirus (HCMV) infection.<sup>20–23</sup> Throughout untreated HIV infection, V $\delta$ 2 T cells exhibit substantially diminished capacity for proliferation, cytokine secretion, cytotoxicity and expression of cytotoxic mediators.<sup>24–31</sup> Although ART may partially re-establish normal V $\delta$ 1:V $\delta$ 2 ratios,  $\gamma\delta$  T cells remain highly activated, and there are conflicting reports of the extent to which  $\gamma\delta$  T cell function is restored.<sup>25,26,30,32–39</sup>

One potential mediator of  $\gamma\delta$  T cell dysfunction is the expression of immune checkpoint molecules (ICMs). During chronic viral infections, persistent antigen exposure drives ICM expression on lymphocytes, including PD-1, TIGIT, Tim-3, CD160 and 2B4. While expression of these markers can reflect a state of immune exhaustion, the functional impact of ICM expression can vary across cellular subsets. Engagement of CD160 on NK cells induces potent effector functions, even in the context of HIV infection,<sup>40–43</sup> while there are contradictory reports of the inhibitory or activating nature of signalling through Tim-3 and TIGIT.<sup>44–53</sup> Currently, the impact of ICM expression on  $\gamma\delta$  T cells remains poorly defined, both at steady-state and in the context of HIV infection.<sup>54,55</sup>

In addition to CD8<sup>+</sup> T cells and NK cells,  $\gamma\delta$  T cells are intriguing candidates for targeting HIV-infected cells in HIV cure strategies. While both  $\gamma\delta$  T cell subsets play an important role in sensing HIV-infected cells,<sup>56–58</sup> the V $\delta$ 2 T cell subset is a particularly interesting immunotherapeutic tool and may contribute to elimination of reactivated HIV-infected cells upon latency reversal.<sup>57,59</sup> The magnitude of and relative ease by which V $\delta$ 2 T cells can be expanded *in vitro* or *in vivo* through application of aminobisphosphonates makes this subset suitable for clinical applications, and human trials involving both allogeneic and autologous V $\delta$ 2 T cell-based immunotherapies targeting various cancer types have revealed acceptable safety profiles.<sup>60–63</sup> The V $\delta$ 1 T cell subset also holds potential for HIV immunotherapies, with expansion protocols for Delta One T (DOT) cells providing opportunities for clinical manipulation.<sup>64</sup> V $\delta$ 1 T cells are capable of antibody-dependent cellular cytotoxicity (ADCC) upon Fc $\gamma$ RIII (CD16) ligation,<sup>65–67</sup> suggesting V $\delta$ 1 T cells could facilitate antibody-mediated killing of HIV-infected cells upon infusion of broadly neutralising antibodies (BnAbs).<sup>68</sup> Furthermore, cytotoxic natural killer receptors (NKR) such as NKG2C are also elevated on V $\delta$ 1 T cells within HIV infection and may contribute substantially to target cell recognition.<sup>69</sup>

Strategies involving  $\gamma\delta$  T cell-mediated elimination of HIV-infected cells must first address gaps in knowledge including mechanisms of infected cell recognition and the impact of ICMs on cytotoxicity pre- and post-expansion. Therefore, we assessed frequency and phenotype of V $\delta$ 1 and V $\delta$ 2 T cells in the context of chronic ART-suppressed HIV infection, characterised the functional capacity and defined the impact of ICM expression on effector functions of both subsets. We additionally explore the *in vitro* expansion of V $\delta$ 2 T cells from PLWH on ART and the mechanisms by which such expanded cells may sense and kill HIV-infected targets. Findings here not only elucidate the impact of chronic infection and ART treatment on  $\gamma\delta$  T cell subsets but also aid in a path towards  $\gamma\delta$  T cell-based immunotherapies within chronic viral infections such as HIV.

## RESULTS

### V $\delta$ 1 T cells are enriched for ICMs and markers of NK cell function in ART-suppressed PLWH

To assess the extent to which suppressive ART reconstitutes both the frequency and phenotype of

$\gamma\delta$  T cells, we analysed circulating V $\delta$ 1 and V $\delta$ 2 T cells among a cohort of 25 PLWH on ART and 17 age-matched uninfected (UI) controls (Supplementary table 1, Supplementary figure 1a, b). The subset of PLWH/ART donors used for phenotyping had been receiving ART treatment for a median 51 months, were virally suppressed ( $< 100$  copies mL $^{-1}$ ), with CD4 $^{+}$  T cell counts above 250  $\mu$ L $^{-1}$ . Despite reconstitution of CD4 T cells, PLWH exhibited persistent expansion of V $\delta$ 1 T cells (median 0.6% UI; 2.3% ART,  $P = 0.003$ ) and concurrent depletion of V $\delta$ 2 T cells (median 1.3% UI; 0.5% ART,  $P = 0.006$ ) relative to UI controls (Figure 1a and b). Consistent with previous reports,<sup>17,35,55,70</sup> we observed an inversion of the peripheral blood V $\delta$ 2:V $\delta$ 1 T cell ratio in PLWH/ART (median 2.35 UI; 0.22 ART,  $P < 0.0001$ ) (Figure 1b).

To determine whether perturbations of V $\delta$ 1 T cells were associated with elevated expression of ICMs, we assessed expression of 2B4, CD160, PD-1, Tim-3 and TIGIT. We observed significantly elevated expression of 2B4 (median 79.1% UI; 97.5% ART), CD160 (median 36.2% UI; 65.5% ART), Tim-3 (median 9.6% UI; 35.2% ART) and TIGIT (median 41.5% UI; 51.3% ART) in PLWH/ART compared to the age-matched UI controls (Figure 1c and d,  $P < 0.05$  for all). Conversely, PD-1 expression was significantly reduced in PLWH/ART (median 45.5% UI; median 25.1% ART,  $P = 0.033$ ) (Figure 1c).

V $\delta$ 1 T cells of PLWH on ART also displayed increased expression of several NK-cell receptors involved in activation and effector function, such as CD94 (median 5.1% UI; 16.2% ART,  $P = 0.010$ ), CD16 (median 13.5% UI; 44.1% ART,  $P < 0.0001$ ) and NKG2C (median 6.5% UI; 15.2% ART,  $P = \text{ns}/0.054$ ) (Figure 1e and f). Chronic viral infection has been reported to drive the appearance of highly differentiated CD16 $^{+}$  CD27 $^{\text{dim/}^{-}}$  V $\delta$ 1 T cells, which, similar to NK cells, can co-express NKG2C and CD57.<sup>65,71</sup> We similarly observed significantly elevated frequencies of CD16 $^{+}$  NKG2C $^{+}$  (median 2.2% UI; 4.9% ART) and highly differentiated CD16 $^{+}$  NKG2C $^{+}$  CD57 $^{+}$  (median 0.8% UI; 3.5% ART) V $\delta$ 1 T cells in the ART group in comparison to healthy controls (Figure 1g). Notably, Tim-3 expression was highly enriched among CD16 $^{+}$  V $\delta$ 1 T cells (median 60.8%, 3.75-fold increase over CD16 $^{-}$ ), with further enrichment among CD16 $^{+}$  NKG2C $^{+}$  CD57 $^{+}$  subsets (median 64.7%, 3.99-fold increase from CD16 $^{-}$ ) (Figure 1h and i). These data suggest that, in a manner analogous to NK cells,<sup>50,53,72</sup> Tim-3 expression may be associated with the maturation

and differentiation of cytotoxic V $\delta$ 1 T cells in ART-treated PLWH.

### V $\delta$ 1 T cells exhibit an NK cell-like functional program during ART-treated HIV

Having observed persistent phenotypic changes and the presence of differentiated NK-like subsets of V $\delta$ 1 T cells in the ART cohort, we next asked whether these were associated with impaired functional responses. To do so, CD3 or CD16 were crosslinked to the murine Fc $\gamma$ R expressing P815 cell line using monoclonal antibodies on a subset of 12 donors from the PLWH/ART cohort. We measured expression of CD69 and CD107a on CD27 $^{\text{dim/}^{-}}$  V $\delta$ 1 T cells (excluding the CD27 $^{\text{hi}}$  naïve-like subset) (Figure 2a–d, Supplementary figure 2a, b), confirming that both CD3 and CD16 crosslinking were sufficient to trigger both activation and degranulation relative to an isotype control.

Given the elevated expression of 2B4, CD160, Tim-3, TIGIT, NKG2C on V $\delta$ 1 T cells within the ART group, we assessed whether receptor ligation could mediate inhibitory or activating signals in the context of CD16-mediated activation. CD16-mediated activation and degranulation were significantly inhibited upon additional crosslinking of Tim-3 (median 1.05-fold decrease CD69,  $P = 0.034$ ; 1.57-fold decrease CD107a,  $P = 0.006$ ) and TIGIT (median 1.37-fold decrease CD69,  $P = 0.001$ ; 3.60-fold decrease CD107a,  $P = 0.004$ ) (Figure 2e–g). In contrast, degranulation (but not activation) could be marginally enhanced upon CD16-crosslinking with either 2B4 or NKG2C (Figure 2h and i), while CD160 or PD-1 crosslinking had no impact (Figure 2j, Supplementary figure 3a, b). CD3-mediated functions followed a similar trend, with activation and degranulation inhibited by Tim-3 and TIGIT (Supplementary figure 3c–l). Overall, V $\delta$ 1 T cells from PLWH/ART were functionally competent, could mediate CD16-dependent degranulation and could be negatively regulated through ligation of Tim-3 and TIGIT.

### Perturbations in V $\delta$ 2 T cell memory states are partially reconstituted in ART-suppressed PLWH

We next characterised the phenotype and function of V $\delta$ 2 T cells within ART-treated PLWH (Supplementary figure 1a, c). Interestingly, we observed that Tim-3 (median 2.5% UI; 13.5% ART) was the only ICM differentially expressed on V $\delta$ 2

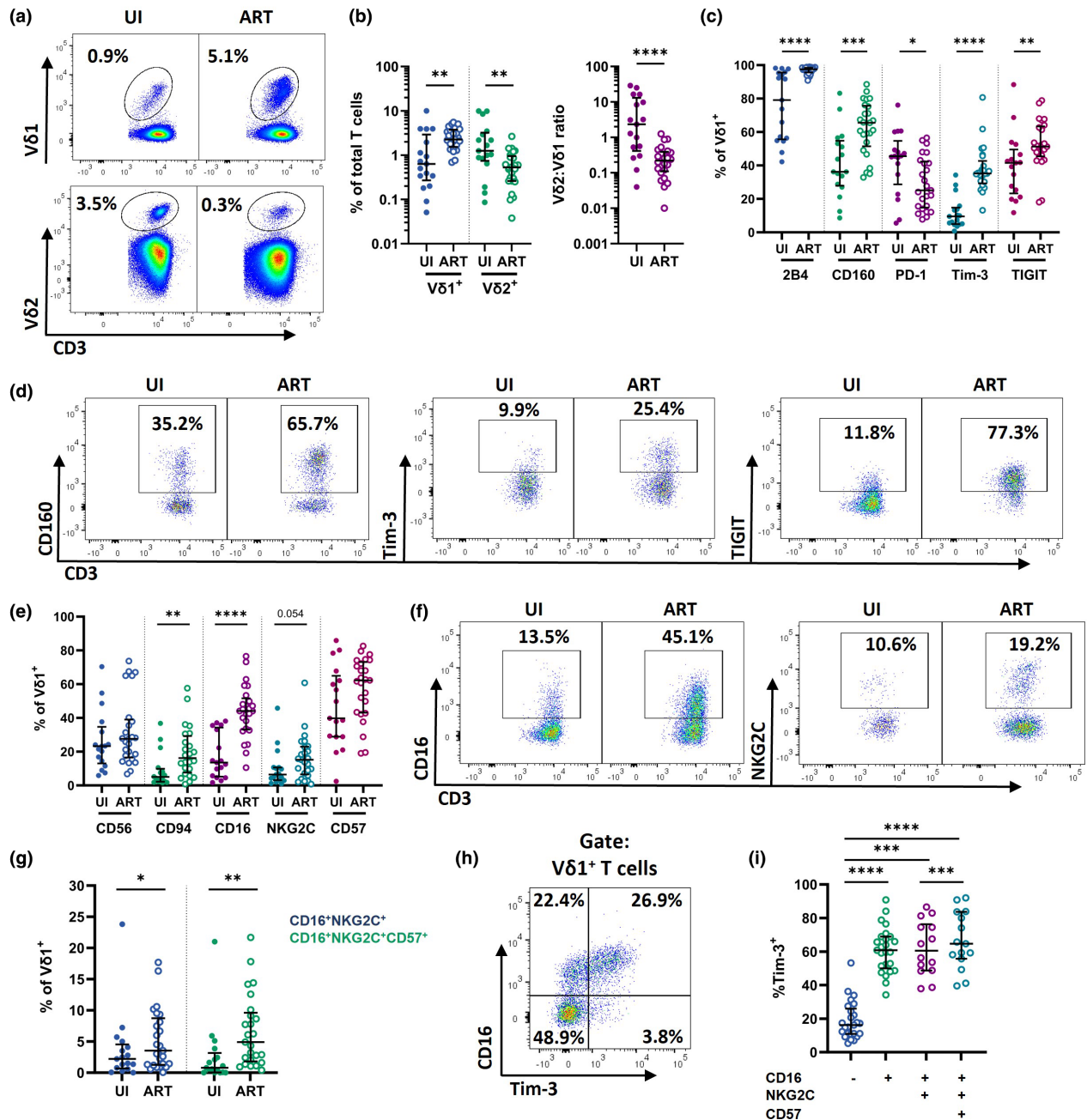


**Figure 1.** Vδ1 T cell phenotypes during chronic ART-treated HIV. **(a)** Representative staining and quantification of Vδ1<sup>+</sup> and Vδ2<sup>+</sup> frequencies and **(b)** ratios within total T cells in PLWH/ART and UI. **(c)** Quantification of 2B4, CD160, PD-1, Tim-3 and TIGIT expression and **(d)** representative staining of CD160, Tim-3 and TIGIT on Vδ1<sup>+</sup> T cells in UI and PLWH/ART. **(e)** Quantification of CD56, CD94, CD16, NKG2C and CD57 expression and **(f)** representative staining of CD16 and NKG2C on Vδ1<sup>+</sup> T cells in UI and PLWH/ART. **(g)** %CD16<sup>+</sup> NKG2C<sup>+</sup> and %CD16<sup>+</sup> NKG2C<sup>+</sup> CD57<sup>+</sup> Vδ1<sup>+</sup> T cells from UI and PLWH/ART. **(h)** Representative plot depicting co-expression of CD16 and Tim-3 on Vδ1<sup>+</sup> T cells in PLWH/ART. **(i)** Tim-3 expression on Vδ1<sup>+</sup> T cells by maturation status in PLWH/ART. Data represents median with IQR. Each datapoint represents results from an individual donor (UI *n* = 17, ART *n* = 26, except **(i)**, where *n* = 16 for CD16<sup>+</sup> NKG2C<sup>+</sup> and CD16<sup>+</sup> NKG2C<sup>+</sup> CD57<sup>+</sup>). Statistics were assessed by Mann–Whitney *U*-tests, except for **(i)**, where statistics were assessed by Wilcoxon matched-pair signed rank test. \**P* < 0.05; \*\**P* < 0.01; \*\*\**P* < 0.001; \*\*\*\**P* < 0.0001. ART, antiretroviral therapy; PLWH, people living with HIV; UI, uninfected individuals.



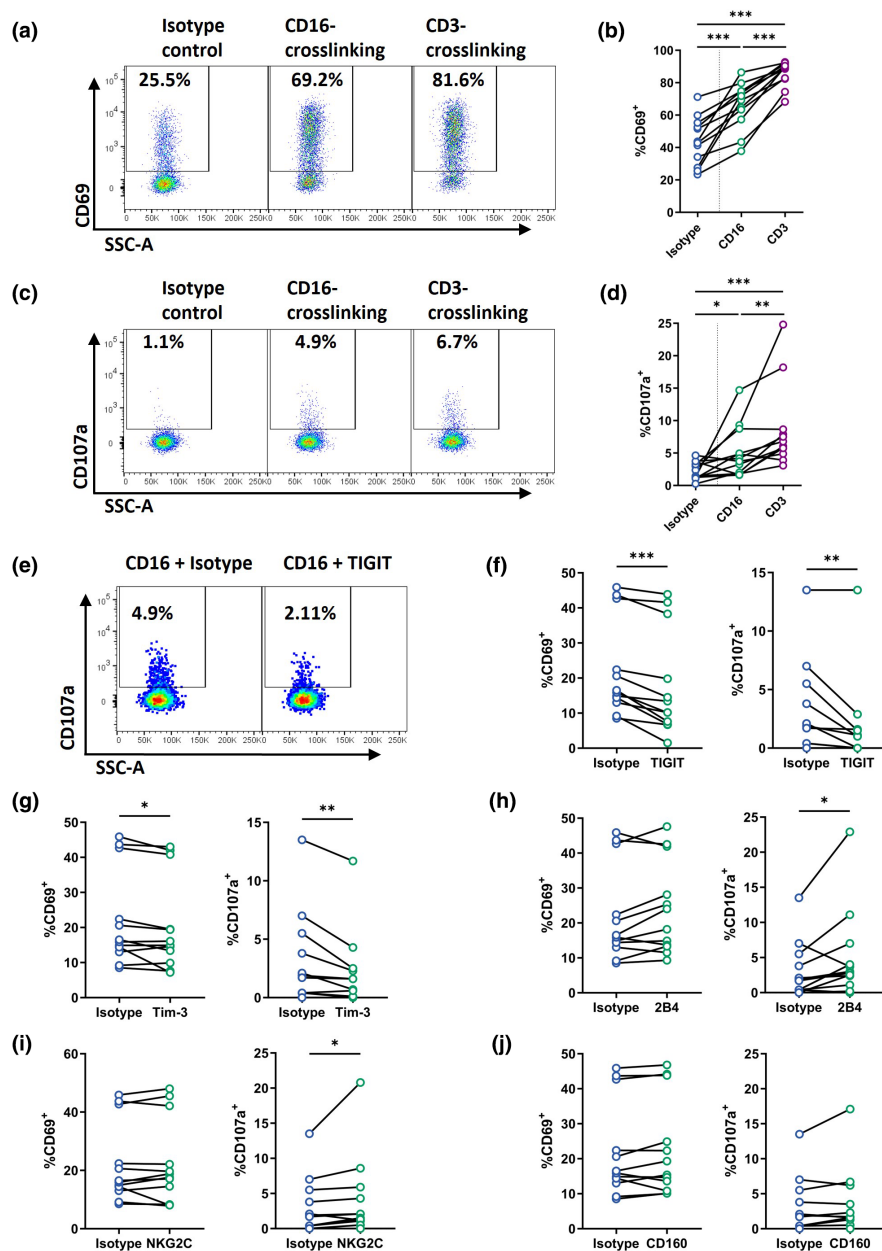


**Figure 2.** V $\delta$ 1 T cell effector functions during chronic ART-treated HIV. Representative staining and quantification of (a, b) CD69 and (c, d) CD107a expression on CD27<sup>dim/-</sup> V $\delta$ 1<sup>+</sup> T cells within PBMC of PLWH/ART upon isotype, CD3 or CD16 crosslinking with P815 cells. (e) Representative staining and (f) quantification of CD107a and CD69 expression on CD27<sup>dim/-</sup> V $\delta$ 1<sup>+</sup> T cells within PBMC of PLWH/ART upon P815 cell crosslinking with CD16 plus either an isotype control or TIGIT. Frequency of CD69 and CD107a expression on CD27<sup>dim/-</sup> V $\delta$ 1<sup>+</sup> T cells within PBMC of PLWH/ART upon concurrent crosslinking of P815 cells with CD16 plus either (g) Tim-3, (h) 2B4, (i) NKG2C or (j) CD160. Values for (f–j) are background subtracted using an isotype only control condition. Each datapoint represents results from an individual donor ( $n = 12$ ). Statistics were assessed by the Wilcoxon matched-pairs signed rank test. \* $P < 0.05$ ; \*\* $P < 0.01$ ; \*\*\* $P < 0.001$ . ART, antiretroviral therapy; PLWH, people living with HIV.

T cells among PLWH/ART in comparison to uninfected controls (Figure 3a and b). Contrastingly, we found V $\delta$ 2 T cells from both UI and PLWH/ART groups expressed similarly high levels of 2B4, CD160

and PD-1, with a substantial degree of variability between donors within the two cohorts (Figure 3a), while TIGIT expression was generally minimal across both groups. The impact of chronic infection on the

differentiation state of Vδ2 T cells was also apparent, with those from the ART group more frequently taking on a T central memory (TCM)-like CD27<sup>+</sup> CD45RA<sup>-</sup> phenotype (median 51.5% UI; 68.9% ART), and less frequently exhibiting a T naïve (Tn)-like CD27<sup>+</sup> CD45RA<sup>+</sup> phenotype (median 22.4% UI; 13.3% ART) (Figure 3c and d). Given the significantly elevated expression of Tim-3 among the ART cohort, we assessed its expression across memory subsets. Tim-3 expression was elevated on Tn (median 3.4 UI; 10.6% ART,  $P = 0.003$ ), TCM (median 1.1% UI; 6.9% ART,  $P < 0.0001$ ) and TEM-like (median 2.9% UI; 16.9% ART,  $P = \text{ns}/0.055$ ) Vδ2 T cell subsets in PLWH/ART compared to uninfected controls, with the most pronounced expression on TEMRA-like CD27<sup>-</sup> CD45RA<sup>+</sup> cells (median 7.3% UI; 42.3% ART,  $P = 0.002$ ) (Figure 3e).

### Vδ2 T cells from ART-treated PLWH exhibit impaired sensitivity to low-dose HMB-PP stimulation

To investigate whether the residual Vδ2 population was functionally competent in the PLWH/ART

group, we stimulated PBMC from a subset of eight PLWH/ART patients with the potent bacterial phosphoantigen (E)-4-hydroxy-3-methyl-but-2-enyl pyrophosphate (HMB-PP) and compared responses with age-matched healthy controls (Supplementary figure 4a–c). Activation (CD69) and degranulation (CD107a) were measured after 5 h of *in vitro* stimulation and varied substantially across individuals (Figure 4a–c). Nonetheless, Vδ2 T cell responses among the ART cohort were negligible at the lowest HMB-PP dose tested (0.02 ng mL<sup>-1</sup>), with only three out of the eight individuals exhibiting responses above background (Figure 4b and c). This stands in contrast to the healthy control donors, where 100% of participants exhibited responses. Furthermore, degranulation of Vδ2 T cells was significantly reduced in the ART cohort at HMB-PP concentrations up to 2 ng mL<sup>-1</sup> (median 23.8% UI vs. 7.1% ART,  $P = 0.021$ ; Figure 4b), with incomplete restoration even at 20 ng mL<sup>-1</sup> (median 24.8% UI; 9.7% ART,  $P = \text{ns}/0.105$ ; Figure 4b). Interestingly, Vδ2 T cells from PLWH/ART were not fully refractory to activation, as HMB-PP-induced CD69 expression

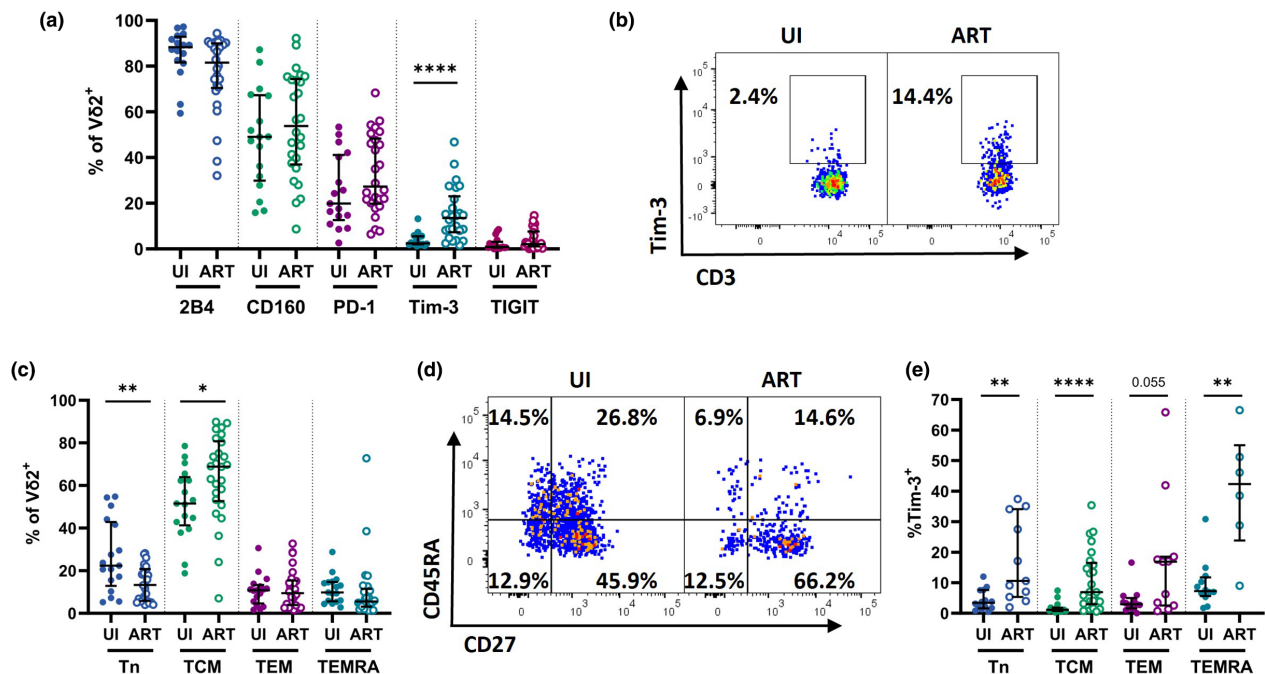


**Figure 3.** Impact of chronic ART-treated HIV infection on Vδ2 T cell phenotypes. **(a)** Quantification and **(b)** representative staining of 2B4, CD160, PD-1, Tim-3 and TIGIT on Vδ2<sup>+</sup> T cells in UI and PLWH/ART. **(c)** Quantification and **(d)** representative staining of Tn (CD27<sup>+</sup> CD45RA<sup>+</sup>), TCM (CD27<sup>+</sup> CD45RA<sup>-</sup>), TEM (CD27<sup>-</sup> CD45RA<sup>-</sup>) and TEMRA (CD27<sup>-</sup> CD45RA<sup>+</sup>) on Vδ2<sup>+</sup> T cells in UI and PLWH/ART. **(e)** Tim-3 expression on Tn, TCM, TEM and TEMRA Vδ2<sup>+</sup> T cell subsets. Data represents median with IQR. Each datapoint represents results from an individual donor ((a, c) UI  $n = 17$ , ART  $n = 27$ , (e)  $n = 6$ –27, depending on cell number). Statistics were assessed by Mann–Whitney  $U$ -tests. \* $P < 0.05$ ; \*\* $P < 0.01$ ; \*\*\* $P < 0.001$ ; \*\*\*\* $P < 0.0001$ . ART, antiretroviral therapy; PLWH, people living with HIV; UI, uninfected individuals.

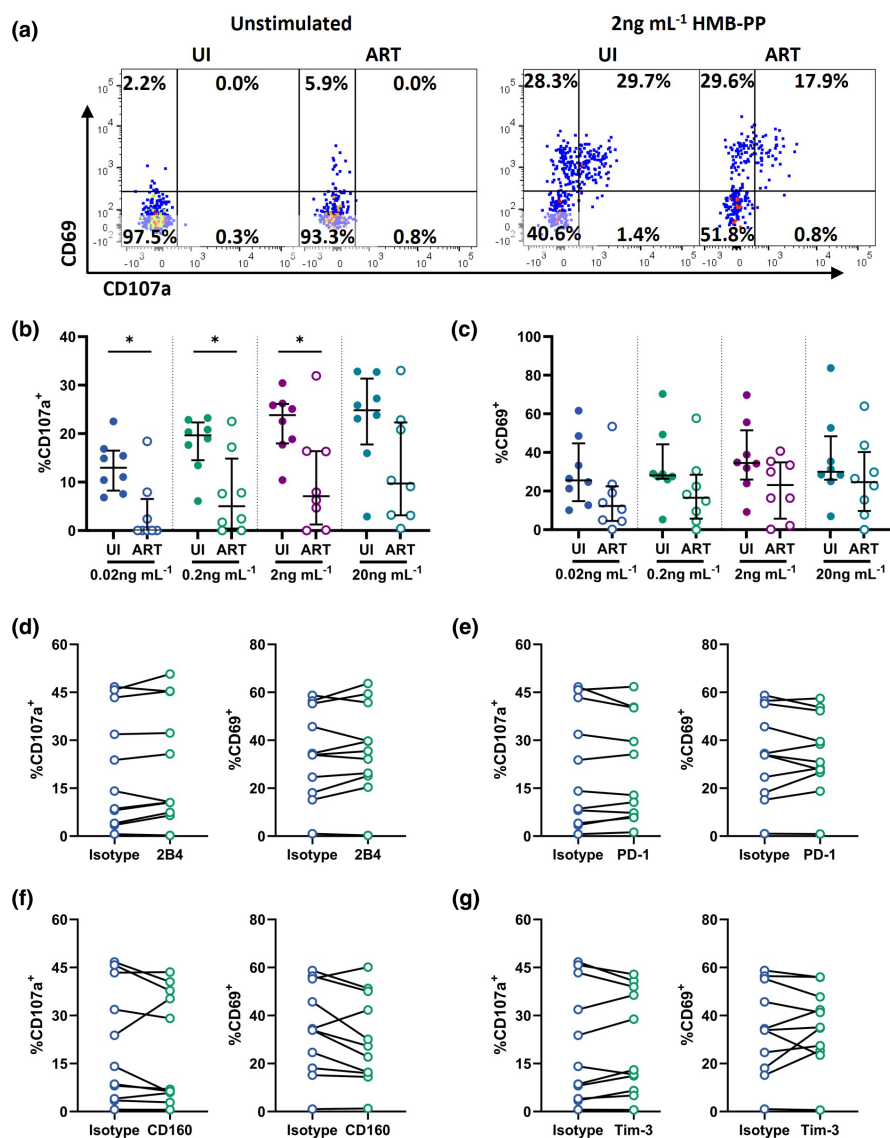


**Figure 4.** HMB-PP induced activation of V $\delta$ 2 T cells within ART-treated PLWH. **(a)** Representative staining of CD107a and CD69 expression on V $\delta$ 2<sup>+</sup>V $\gamma$ 9<sup>+</sup> T cells within PBMC of PLWH/ART or UI donors either unstimulated or upon stimulation with 2 ng mL<sup>-1</sup> HMB-PP. Quantification of **(b)** CD107a<sup>+</sup> and **(c)** CD69<sup>+</sup> expressing V $\delta$ 2<sup>+</sup>V $\gamma$ 9<sup>+</sup> T cells after *in vitro* stimulation of whole PBMC from PLWH/ART or UI with 0.02 ng mL<sup>-1</sup>, 0.2 ng mL<sup>-1</sup>, 2 ng mL<sup>-1</sup> or 20 ng mL<sup>-1</sup> HMB-PP. Data represents median with IQR. Each datapoint represents results from an individual donor ( $n = 8$  UI,  $n = 8$  ART). Statistics were assessed Mann–Whitney *U*-tests. \* $P < 0.05$ . The impact of blocking **(d)** 2B4, **(e)** PD-1, **(f)** CD160 or **(g)** Tim-3 on %CD107a<sup>+</sup> and %CD69<sup>+</sup> V $\delta$ 2<sup>+</sup> T cells within PBMC of PLWH/ART upon 0.2 ng mL<sup>-1</sup> HMB-PP stimulation. Each datapoint represents results from an individual donor ( $n = 11$ ). Statistics were assessed by the Wilcoxon matched-pairs signed rank test. ART, antiretroviral therapy; HMB-PP, (E)-4-hydroxy-3-methyl-but-2-enyl pyrophosphate; PLWH, people living with HIV; UI, uninfected individuals.

was more comparable between groups (Figure 4c), although there was a trend towards lower activation for the PLWH/ART group.

As 2B4, CD160, PD-1 and Tim-3 were all expressed on V $\delta$ 2 T cells within the cohort of PLWH on ART, we assessed whether inhibitory signalling through these receptors could be contributing to impaired HMB-PP responsiveness. HMB-PP-mediated V $\delta$ 2

responsiveness was not impacted by blocking with monoclonal antibodies against any of the ICMs, with no significant changes in expression of either CD69 or CD107a (Figure 4d–g). Therefore, we conclude that it is unlikely that the impaired responsiveness to HMB-PP *ex vivo* observed in PLWH/ART is because of differential expression of ICMs between these cohorts.

### V $\delta$ 2 T cells from ART-treated PLWH exhibit a reduced capacity for *in vitro* expansion

*In vitro* or *in vivo*-expanded V $\delta$ 2 T cells are a potential immunotherapeutic tool for the treatment of a number of infectious diseases. In line with this, we assessed whether ART-suppressed chronic HIV infection impacts the expansion potential of V $\delta$ 2 T cells, and whether such expanded cells were capable of targeting HIV-infected cells. PBMC from a subset of 16 PLWH/ART were treated with zoledronate plus IL-2 to induce *in vitro* expansion of V $\delta$ 2 T cells.

The cellular composition of cultures was assessed by flow cytometry on day 10 or 11 (Supplementary figure 5a). V $\delta$ 2 expansion was poor in nine out of the 16 PLWH/ART, where V $\delta$ 2 T cells composed < 60% of the resultant culture (Figure 5a). In contrast, expansion from healthy donors which resulted in cultures with median frequencies of about 80–92.1% V $\delta$ 2<sup>+</sup> CD3<sup>+</sup> (Supplementary figure 5b).<sup>73</sup> Contaminating cells in expansions from PLWH/ART were largely  $\alpha\beta$  T cells (median 18.2%) and CD3<sup>−</sup> CD56<sup>+</sup> NK cells (median 10.6%) (Figure 5b). The best correlate of V $\delta$ 2 expansion for PLWH/ART donors was the

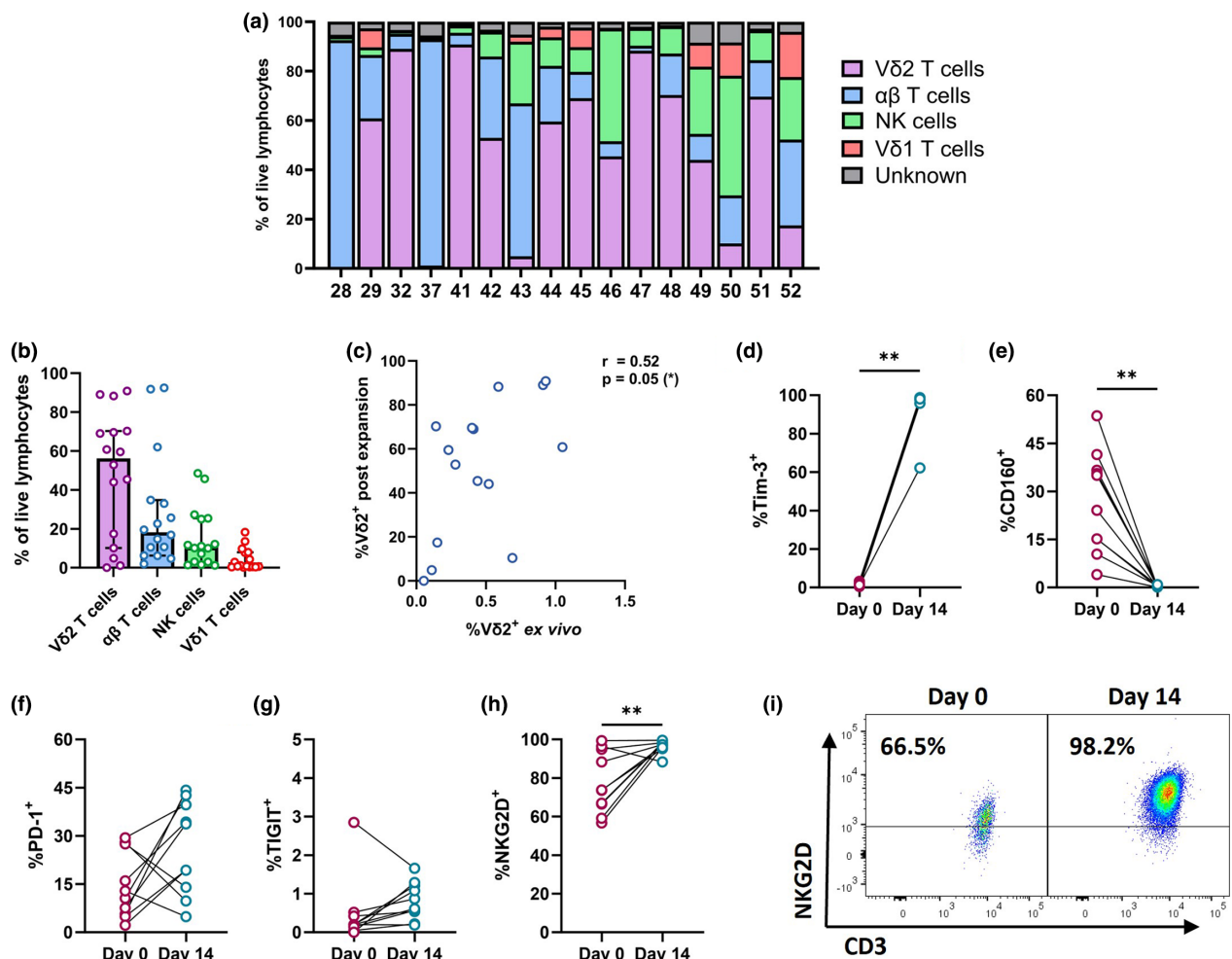


**Figure 5.** Phenotype of expanded V $\delta$ 2 T cells from PLWH on ART. **(a, b)** Frequency of V $\delta$ 2<sup>+</sup> CD3<sup>+</sup>, V $\delta$ 1<sup>+</sup> CD3<sup>+</sup>,  $\alpha\beta$  TCR<sup>+</sup> CD3<sup>+</sup>, CD56<sup>+</sup> CD3<sup>−</sup> (NK cells) or undefined cells as a proportion of total live lymphocytes within cultures from PLWH/ART after 10/11 days of zoledronate and IL-2-mediated *in vitro* expansion. **(c)** Correlation between %V $\delta$ 2<sup>+</sup> T cells pre-expansion and %V $\delta$ 2<sup>+</sup> T cells on day 10/11 of *in vitro* expansion. Expression of **(d)** Tim-3, **(e)** CD160, **(f)** PD-1 and **(g)** TIGIT on V $\delta$ 2<sup>+</sup> T cells from PLWH/ART pre-expansion (day 0) or after 14 days of *in vitro* expansion. **(h)** Quantification and **(i)** representative staining of NKG2D expression on V $\delta$ 2<sup>+</sup> T cells from PLWH/ART pre-expansion (day 0) or after 14 days of *in vitro* expansion. Data represents median with IQR. Each datapoint represents results from an individual donor (**(a–c)**  $n = 16$ , **(d–h)**  $n = 10$ ). Statistics were assessed by the Wilcoxon matched-pairs signed rank test. Correlations were calculated with Spearman's  $r$  with two-tailed post-tests. \* $P < 0.05$ ; \*\* $P < 0.01$ . ART, antiretroviral therapy; PLWH, people living with HIV.



baseline frequency of V $\delta$ 2 T cells in PBMC (Spearman's  $r$  0.52;  $P$  = 0.05) (Figure 5c), rather than any markers of V $\delta$ 2 T cell differentiation (Supplementary figure 5c, d). We next assessed the modulation of ICM expression during *in vitro* expansion (Supplementary figure 6a, b). Expanded V $\delta$ 2 T cells exhibited near-universal up-regulation of Tim-3 (median 0.8% day 0; 97.4% day 14) coupled with near-total loss of CD160 (median 29.6% day 0; 0.3% day 14) (Supplementary figure 6b, Figure 5d and e). Neither PD-1 nor TIGIT expression were significantly modulated during expansion (Figure 5f and g). Finally, we assessed expression of NKG2D, a surface receptor known to contribute substantially to V $\delta$ 2 T cell-mediated cytotoxicity, which may be involved in the recognition of HIV-infected cells. The frequency of NKG2D<sup>+</sup> V $\delta$ 2 T cells was significantly increased after *in vitro* expansion (median 73.7% day 0; 97.7% day 14,  $P$  = 0.010) (Figure 5h and i).

### Expanded V $\delta$ 2 T cells from ART-treated PLWH maintain efficient anti-HIV effector functions

To assess whether expanded V $\delta$ 2 T cells maintain anti-HIV effector functions in ART-suppressed chronic HIV infection, we performed infected cell elimination (ICE) assays against the 8E5/LAV cell line, a CEM-derived cell line that contains a single copy of the HIV provirus.<sup>74,75</sup> Importantly, cultures of 8E5 cells contain a mix of provirus transcribing cells and cells that have lost the ability to produce viral antigens. Detection of the p24 antigen via flow cytometry allows identification of HIV transcribing cells in such mixed cultures.<sup>76</sup> Lysis of p24<sup>+</sup> (HIV antigen expressing) or p24<sup>-</sup> (non-antigen expressing) 8E5 cells was measured after a 4-h co-incubation with expanded V $\delta$ 2 T cells at effector to target (E:T) cell ratios of 5:1, 2:1, 1:1, 1:2, 1:5 and 1:10 (Supplementary figure 7a). Expanded V $\delta$ 2 T cell cultures from PLWH/ART containing less than 70% V $\delta$ 2 T cells were depleted of contaminating  $\alpha\beta$  and/or V $\delta$ 1 T cells prior to use in ICE assays (Supplementary figure 7b).

Despite the persistent defects in *ex vivo* responsiveness to HMB-PP, V $\delta$ 2 T cells from the ART group efficiently eliminated HIV-infected cells (Figure 6a). At the highest E:T ratio tested (5:1), expanded V $\delta$ 2 T cells from uninfected donors demonstrated considerable cytotoxicity against infected (p24<sup>+</sup>) cells (median 80.6%; Figure 6b). V $\delta$ 2 T cells expanded from PLWH/ART also displayed

substantial elimination of p24<sup>+</sup> 8E5 cells (median 94.4%; Figure 6a). Impressively, V $\delta$ 2 T cells expanded from PLWH/ART were still able to efficiently kill infected cells at the 1:10 E:T ratio (median 16.0%). Furthermore, p24<sup>+</sup> cells were preferentially killed, with a lower level of cytotoxicity against the p24<sup>-</sup> 8E5 cells, and minimal killing of the uninfected parental like CEM.NKR CCR5 cell line (Supplementary figure 7c). These data indicate HIV infection of this cell line is likely contributing to recognition by V $\delta$ 2 T cells, which is further elevated upon transcription of viral antigens.

To determine the mechanism of infected cell elimination, we first examined expression of ligands for the key V $\delta$ 2 T cell cytotoxic surface receptors DNAM-1, 2B4 and NKG2D on 8E5 target cells using Fc-chimera proteins (Supplementary figure 8a). As the ligands for 2B4 and NKG2D, but not DNAM-1, were expressed to high degrees on target cells (Supplementary figure 8b–d), we next blocked 2B4 or NKG2D within the infected cell elimination assay at E:T ratios of 1:1. Here, we observed that blocking NKG2D significantly diminished the targeting of both p24<sup>+</sup> (median 24.79% decrease UI, median 58.36% decrease ART) and p24<sup>-</sup> (median 15.94% decrease UI, median 46.35% decrease ART) cells by expanded V $\delta$ 2 T cells when compared to an isotype control (Figure 6c and d), suggesting the NKG2D surface receptor contributes substantially to recognition of HIV-infected cells by expanded V $\delta$ 2 T cells.

## DISCUSSION

Although ART efficiently suppresses viral replication and reconstitutes CD4 T cell counts, ongoing inflammation and incomplete restoration of immune function results in persistently elevated risk of co-morbidities and co-infections such as TB.<sup>77,78</sup> The extent to which perturbations within the  $\gamma\delta$  T cell compartment are restored following ART is understudied, despite the potential importance of  $\gamma\delta$  T cells as an immunotherapy tool. Here, we report persistence of highly differentiated V $\delta$ 1 T cells despite ART-mediated viral suppression, with elevated expression of ICMs such as Tim-3 and TIGIT that were found to suppress effector functions. V $\delta$ 2 T cell reactivity to phosphoantigen stimulation remained diminished within ART-treated individuals; however, no link between ICM expression and reduced responsiveness could be identified. Despite residual perturbations in

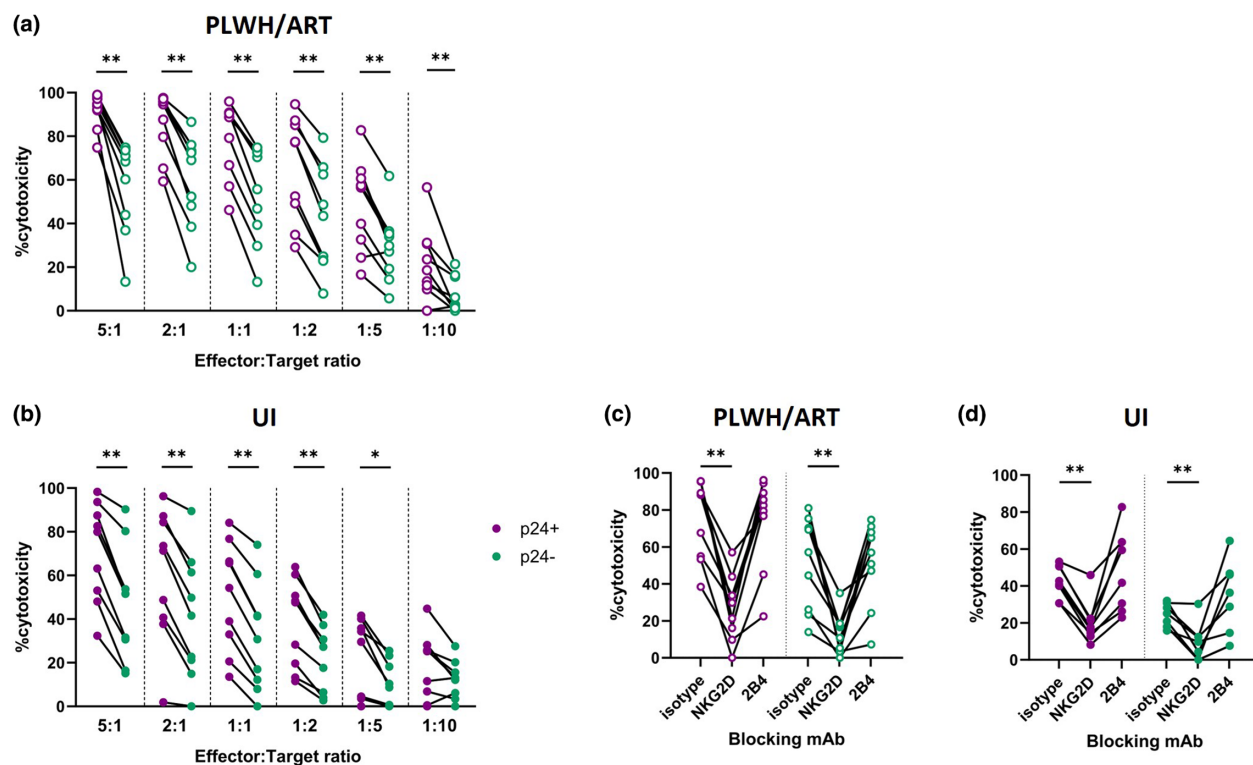


**Figure 6.** Elimination of HIV-infected cells by expanded V $\delta$ 2 T cells from PLWH on ART or UI. Elimination of p24<sup>+</sup> (purple) or p24<sup>-</sup> (green) 8E5 cells by expanded V $\delta$ 2 T cells. Cytotoxic capacity of V $\delta$ 2 T cells expanded from (a) PLWH/ART and (b) UI at E:T ratios of 5:1, 2:1, 1:1, 1:2, 1:5 or 1:10. Impact of blocking antibodies against an isotype control, NKG2D or 2B4 at an E:T ratio of 1:1 with V $\delta$ 2 T cells expanded from (c) PLWH/ART and (d) UI. Each datapoint represents results from an individual donor ( $n = 9$ ). Statistics were assessed by the Wilcoxon matched-pairs signed rank test. \* $P < 0.05$ ; \*\* $P < 0.01$ . ART, antiretroviral therapy; E:T, effector:target; PLWH, people living with HIV; UI, uninfected individuals.

phenotypes, both V $\delta$ 1 and V $\delta$ 2 T cell subsets from PLWH on ART exhibited a strong capacity for anti-HIV effector functions, highlighting their potential for use within future immunotherapies or HIV curative strategies.

During untreated HIV infection, viral replication in the gut-associated lymphoid tissue (GALT) damages the mucosal epithelia, allowing translocation of microbial products into the circulation and driving systemic immune activation.<sup>79–81</sup> Previous studies have suggested that microbial translocation is involved in V $\delta$ 1 T cell expansion, activation, proinflammatory cytokine production<sup>31,82–85</sup> and terminal differentiation.<sup>25,82,85–87</sup> Notably, Fausther-Bovendo *et al.* (2008) reported a loss of NKG2A and acquisition of NKG2C expression on V $\delta$ 1 T cells from untreated PLWH, finding NKG2C to contribute substantially to V $\delta$ 1-mediated elimination of HIV-infected CD4<sup>+</sup> T cells.<sup>69</sup> Similar observations have been reported in elite controller (EC) cohorts,<sup>82,85</sup> where PLWH maintain low or undetectable plasma viraemia but experience persistent viral replication

in, and damage to, the GALT.<sup>88</sup> Our data highlight that, similar to both untreated HIV infection and EC cohorts, PLWH on ART exhibit the persistence of highly differentiated, TEMRA-like V $\delta$ 1 T cells, and demonstrate that the phenotype of these highly differentiated V $\delta$ 1 T cells mirrors that of matured CD16<sup>+</sup> NKG2C<sup>+</sup> and CD16<sup>+</sup> NKG2C<sup>+</sup> CD57<sup>+</sup> NK cell subsets. Similar populations of expanded, cytotoxic V $\delta$ 1 T cell subsets with elevated expression of CD16, CD57 and NKG2C have been described in HCMV infection,<sup>20–23</sup> which is highly prevalent among PLWH (90–100% seropositivity).<sup>89,90</sup> We therefore speculate that the V $\delta$ 1 expansion and differentiation observed during ART is likely to be driven by a combination of HCMV, microbial translocation and inflammatory signals, all of which persist despite effective viral suppression.<sup>79,80,91</sup>

V $\delta$ 1 T cells nonetheless appear to remain highly functional during ART, as demonstrated by the robust CD3- and CD16-driven activation and degranulation observed in our assays, which is consistent with other reports describing the

cytotoxic capacity of V $\delta$ 1 T cells from both treated and untreated HIV infection.<sup>69,92</sup> Data regarding ICM expression and function on  $\gamma\delta$  T cells is sparse and often conflicting; increased expression of PD-1 on V $\delta$ 1 and V $\delta$ 2 T cells has been observed in ART-treated HIV infection,<sup>55</sup> while others report elevated expression of Tim-3, TIGIT and CD160.<sup>54</sup> Here, we find that 2B4, CD160, Tim-3 and TIGIT were expressed by a higher proportion of V $\delta$ 1 T cells in PLWH/ART compared to uninfected controls. In contrast to a previous study,<sup>55</sup> we observed lower PD-1 expression on V $\delta$ 1 T cells in PLWH/ART compared to age-matched uninfected controls. These discrepant results may reflect baseline immunological differences in V $\delta$ 1 T cells or PD-1 expression between the populations studied. Tim-3 and TIGIT were found to suppress CD16-driven effector functions, indicating a potential inhibitory role for these receptors on V $\delta$ 1 T cells. Conversely, we found no evidence of inhibition of CD16-mediated activation or degranulation by PD-1 or CD160. These data, together with the heightened proportions of V $\delta$ 1 T cells within both acute and ART-treated HIV infection, highlight the potential for the engagement of this subset alongside cocktails of broadly neutralising antibodies (BnAbs) to facilitate ADCC of reactivated HIV-infected cells.<sup>68</sup> Additionally, our data suggest that blockade of Tim-3 or TIGIT, or co-stimulation through NKRs such as NKG2C or 2B4, could enhance CD16-mediated effector functions. Further investigations to characterise the potential of V $\delta$ 1 T cell-mediated ADCC of HIV-infected cells, and the utilisation of DOT cells in this context could aid in the search for a functional cure for HIV upon latency reversal.

In contrast to V $\delta$ 1 T cells, V $\delta$ 2 T cell cytokine secretion, phosphoantigen reactivity and cytotoxic capacity are considerably impaired in untreated HIV infection.<sup>17,24–26,28–31</sup> In parallel, increased proportions of terminally differentiated TEMRA-like V $\delta$ 2 T cells have been commonly observed within untreated HIV infection.<sup>17,25,35</sup> Several previous studies have assessed memory subset distribution within ART-treated individuals but report contrasting results regarding the impact of infection on proportions of naïve, central memory or TEMRA populations.<sup>17,35,38,55</sup> In the present study, we found elevated proportions of TCM-like and a decreased frequency of naïve-like V $\delta$ 2 T cells in PLWH/ART compared to age-matched uninfected individuals, while frequencies of TEMRA-like and TEM-like V $\delta$ 2 T cells were similar between groups.

Overall, most evidence suggests that ART treatment may reconstitute proportions of TEMRA-like V $\delta$ 2 T cells; however, perturbations evidently persist within other memory subsets, with a high degree of variation seen between study cohorts, perhaps caused by geographical location, ART regimes or differences in cohort demographics.

Our observation that V $\delta$ 2 T cells from PLWH on ART remained largely unresponsive to phosphoantigen stimulation compared to age-matched controls is similar to earlier reports of continual activation and diminished functionality of V $\delta$ 2 T cells despite viral suppression.<sup>25,30,37–39,55</sup> Blocking ICMs failed to restore sensitivity to low-dose HMB-PP stimulation, and together with our observation that V $\delta$ 2 T cells in the PLWH/ART cohort did not express elevated levels of most ICMs, we conclude that these markers are unlikely to play a significant role in V $\delta$ 2 T cell functions in this context. Of note, Tim-3 expression was found to be significantly heightened on V $\delta$ 2 T cells within PLWH/ART across all memory states and was additionally upregulated upon *in vitro* expansion. As we were unable to find evidence that Tim-3 suppressed HMB-PP-mediated activation, the role of this marker on V $\delta$ 2 T cells remains unclear and should be investigated within future studies. Alternatively, compromised phosphoantigen signalling to V $\delta$ 2 T cells from HIV-infected APCs may contribute to this functional impairment.<sup>93,94</sup> As V $\delta$ 2 T cell phosphoantigen responsiveness is mediated through BTN3A1 and BTN2A1,<sup>95,96</sup> future studies should investigate the impact of acute, chronic and ART-treated HIV infection on the expression of and signalling through these molecules.

Although it was possible to expand V $\delta$ 2 T cells *in vitro* from some donors within the PLWH/ART cohort, expansion was not as reliable or efficient as from uninfected donors. V $\delta$ 2 T cell frequencies *ex vivo* correlated with the success of expansion. This finding could be particularly relevant in the context of therapeutic manipulation of V $\delta$ 2 T cells in cohorts of ART-treated PLWH. Identification of individuals with efficient V $\delta$ 2 T cell expansion capacity will inform choices regarding the use of autologous versus allogeneic immunotherapeutic approaches. Despite the high degree of variability in HMB-PP and/or zoledronate + IL-2 responsiveness, successfully expanded V $\delta$ 2 T cell cultures from PLWH/ART were capable of remarkably potent effector functions against an HIV-infected cell line, with preferential killing of infected cells expressing HIV antigens. Furthermore, we identify

NKG2D-mediated recognition as a key pathway for elimination of HIV-infected cells. HIV infection of primary CD4<sup>+</sup> T cells is known to drive upregulation of the UL16-binding proteins-1 to -3, which are key ligands for NKG2D.<sup>97</sup> Here, we detected high frequencies of NKG2D expressing V $\delta$ 2 T cells from PLWH/ART, which was further increased upon *in vitro* expansion. We conclude that although V $\delta$ 2 T cell TCR/phosphoantigen signalling pathways appear to be compromised in the context of HIV/ART, NKG2D-mediated recognition and activation is not functionally impaired, allowing for efficient elimination of infected cells.

In summary, we explored functional perturbations of  $\gamma\delta$  T cell subsets in PLWH undergoing suppressive ART. We identify that the V $\delta$ 1 T cell subset remains highly differentiated throughout treatment, taking on an NK cell-like phenotype with increased expression of Tim-3 and TIGIT that were found to slightly inhibit effector functions upon crosslinking. Perturbations in V $\delta$ 2 T cell memory phenotypes were partially restored upon effective viral suppression, though phosphoantigen sensitivity was still significantly impaired. Despite persistent phenotypical alterations in ART-treated individuals, both  $\gamma\delta$  T cell subsets maintained robust anti-HIV effector functions, illuminating a pathway towards the inclusion of  $\gamma\delta$  T cell-based approaches within HIV immunotherapies.

## METHODS

### Sample collection and isolation of PBMC from whole blood

Whole blood was collected from a total of 52 people living with HIV undergoing suppressive antiretroviral therapy (PLWH/ART) recruited through the Melbourne Sexual Health Centre between 2012 and 2023. A total of 29 uninfected controls (UI) were recruited at the University of Melbourne. PBMC were isolated from whole blood using Ficoll-Paque gradient density centrifugation (Cytiva, Cambridge, USA) and either used immediately or cryopreserved in freeze solution (90% fetal calf serum (FCS)) (Sigma-Aldrich, St. Louis, USA) and 10% dimethyl sulfoxide (DMSO) (Sigma-Aldrich) for future use.

### Ex vivo phenotypical analysis

Cryopreserved PBMC were thawed in RPMI 1640 medium (Gibco, Waltham, USA) supplemented with 10% FCS and penicillin/streptomycin/l-glutamate (Gibco) (RF10), briefly washed in PBS then stained with:

UV viability dye (ThermoFisher, Scoresby, Australia), Aqua viability dye (ThermoFisher), V $\delta$ 1 FITC (TS8.2; ThermoFisher),

V $\delta$ 2 BV786 (B6; BD Biosciences, San Jose, USA), V $\delta$ 2 PE (B6; Biolegend, San Diego, USA), CD19 BB700 (SJ25C1; BD Biosciences), CD56 BUV737 (NCAM16.2; BD Biosciences), CD3 BV510 (SK7; Biolegend), CD3 BUV805 (SK7; BD Biosciences), CD160 Alexa Fluor-647 (BY55; BD Biosciences), PD-1 BV421 (EH12.2H7; Biolegend), Tim-3 PE-TR (7D3; BD Biosciences), Tim-3 BUV737 (7D3; BD Biosciences), TIGIT APC Fire 750 (A15153G; Biolegend), 2B4 APC Cy7 (C1.7; Biolegend), 2B4 PE-Dazzle (C1.7; Biolegend), CD16 BV650 (3G8; BD Biosciences), NKG2C PE (134 591; R&D Systems, Minneapolis, USA), CD57 BV510 (QA17A04; Biolegend), CD57 PacBlue (HCD57; Biolegend), CD94 APC (HP-3D9; BD Biosciences), CD94 BUV395 (HP-3D9; BD Biosciences), CD45RA FITC (HI100; Biolegend), CD45RA PerCpCy5.5 (HI100; Biolegend), CD27 BV510 (M-T271; Biolegend), CD27 BV786 (L128; BD Biosciences), CD27 BUV737 (L128; BD Biosciences), CD26 FITC (BA5b; Biolegend) and NKG2D BV650 (1D11; BD Biosciences).

After surface staining, cells were washed and resuspended in PBS containing 2% FCS before acquisition on a BD LSR Fortessa using BD FACS Diva. For each memory subset, donors with less than 100 events were excluded from analysis.

### ICM crosslinking of V $\delta$ 1 T cells

Fresh PBMC isolated from PLWH/ART were rested overnight in RF10 at 37°C 5% CO<sub>2</sub>. The next day,  $0.5 \times 10^6$  PBMC were added to a 96-well round bottom plate at a 1:1 ratio with murine P815 cells (ATCC, Manassas, USA) and stimulated with 40 ng mL<sup>-1</sup> of monoclonal antibodies against either CD3 (OKT3; Biolegend), CD16 (3G8; Biolegend) or an isotype control (MOPC-21; Biolegend). 5  $\mu$ g mL<sup>-1</sup> of monoclonal antibodies against either CD160 (BY55; Biolegend), 2B4 (C1.7; Biolegend), Tim-3 (F38-2E2; Biolegend), TIGIT (MBSA43; eBioscience, San Diego, USA), PD-1 (EH12.2H7; Biolegend), NKG2C (134522; R&D Systems) or an isotype control (MOPC-21; Biolegend) were then added to CD3 or CD16 stimulated conditions. CD107a APCH7 (H4A3; BD Biosciences) was added to each well, and the plate was briefly centrifuged before incubation at 37°C with 5% CO<sub>2</sub> for 5 h. After incubation, wells were washed, and cells stained with UV viability dye (ThermoFisher) then a cocktail containing V $\delta$ 1 FITC (TS8.2; Invitrogen, Carlsbad, USA), CD3 BV510 (SK7; Biolegend), CD27 BV650 (0323; Biolegend), CD69 PE Dazzle (FN50; Biolegend) and CD56 BUV737 (NCAM16.2; BD Biosciences). After staining, cells were washed and resuspended in PBS containing 2% FCS before acquisition on a BD LSR Fortessa using BD FACS Diva.

### HMB-PP induced activation of V $\delta$ 2 T cells

Cryopreserved PBMC were thawed in RF10, then rested overnight at 37°C 5% CO<sub>2</sub>. The next day,  $1.0 \times 10^6$  PBMC were added to a 96-well round bottom plate. For ICM blocking experiments, 4  $\mu$ g mL<sup>-1</sup> of blocking antibodies against 2B4 (eBioPP35; eBioscience), PD-1 (EH12.2H7; Biolegend), CD160 (688327; Biolegend), Tim-3 (F38-2E2; Biolegend) or an isotype control (MOPC-21; Biolegend) were added to wells and incubated for 30 min at 37°C 5% CO<sub>2</sub>. HMB-PP (Sigma-Aldrich) was added to wells at a final concentration of either 20 ng mL<sup>-1</sup>, 2 ng mL<sup>-1</sup>, 0.2 ng mL<sup>-1</sup> or 0.02 ng mL<sup>-1</sup>. Some wells were left unstimulated to



assess background activation. CD107a APC7 (H4A3; BD Biosciences) was added to each well before incubation at 37°C 5% CO<sub>2</sub> for 5 h. After incubation, cells were washed then stained with Aqua viability dye (ThermoFisher) and a cocktail containing CD69 FITC (FN50; Biolegend), CD3 BUV805 (SK7; BD Biosciences), plus either V $\delta$ 2 PE (B6; Biolegend) for blocking experiments or V $\gamma$ 9 PE (B3; Biolegend) and V $\delta$ 2 BV786 (B6; BD Biosciences) for HMB-PP titrations. After staining, cells were resuspended in PBS containing 2% FCS before acquisition on a BD LSR Fortessa using BD FACS Diva.

### ***In vitro* expansion of V $\delta$ 2 T cells**

Cryopreserved PBMC were thawed in RF10, then stimulated with 15  $\mu$ M zoledronic acid monohydrate (Sigma-Aldrich) and 100 IU mL<sup>-1</sup> IL-2 (PeproTech, Cranbury, USA) and incubated in 5% CO<sub>2</sub> at 37°C. Every 2–3 days, expansions were washed and resuspended in fresh media supplemented with 100 IU mL<sup>-1</sup> IL-2 at  $2 \times 10^6$  cells mL<sup>-1</sup>.

### **V $\delta$ 2 T cell expansion purity assessment and depletion of contaminating cells**

Expansion from the PLWH/ART cohort was assessed for purity of V $\delta$ 2 T cells on day 10 or 11.  $0.5 \times 10^6$  cells were stained with Aqua viability dye (ThermoFisher), V $\delta$ 1 APC (TS8.2; ThermoFisher), CD3 BV786 (SK7; Biolegend), CD56 BUV395 (NCAM16.2; BD Biosciences), V $\delta$ 2 PE (B6; Biolegend) and TCR  $\alpha\beta$  PE-Cy7 (IP36; ThermoFisher). After staining, cells were resuspended in PBS containing 2% FCS before acquisition before acquiring samples on a BD LSR Fortessa using BD FACS Diva. Contaminating cells were magnetically depleted of TCR  $\alpha\beta$  PE-Cy7 (IP36; ThermoFisher) and/or V $\delta$ 1 PE-Cy7 (TS8.2; ThermoFisher) binding cells using anti-PE MicroBeads (Miltenyi Biotec, Sydney, Australia) according to the manufacturer's instructions. Depleted cultures were again checked for V $\delta$ 2 T cell purity by staining with an Aqua viability dye (ThermoFisher), CD3 BV786 (SK7; Biolegend), CD56 BUV395 (NCAM16.2; BD Biosciences), V $\delta$ 2 PE (B6; Biolegend) and TCR  $\alpha\beta$  PE-Cy7 (IP36; ThermoFisher).

### **Flow cytometry-based infected cell elimination assay**

Lysis of the 8E5/LAV HIV-infected cell line (NIH ARP-#95) was quantified using a modified version of a flow cytometry-based infected cell elimination assay previously described.<sup>74</sup> Expanded V $\delta$ 2 T cells were collected for use on day 12 or 13 of *in vitro* expansion. For surface receptor blocking, expanded V $\delta$ 2 T cells were preincubated with 5  $\mu$ g mL<sup>-1</sup> of anti-NKG2D (1D11; Biolegend), anti-2B4 (eBioPP35; eBioscience) or an IgG1  $\kappa$  isotype control (MOPC-21; Biolegend) for 30 min at 37°C 5% CO<sub>2</sub>. 8E5 target cells were stained with eFluor 670 dye (eBioscience) and added to tubes containing expanded V $\delta$ 2 T cells at effector:target cell ratios of 5:1, 2:1, 1:1, 1:2, 1:5 and 1:10, or to a tube without effector cells to measure background death. For some experiments, eFluor 670 stained CEM.NKr-CCR5 cells (NIH ARP-4376) were used in place of 8E5 cells. Tubes were centrifuged at  $300 \times g$  for 1 min, then

incubated at 37°C with 5% CO<sub>2</sub> for 4 h. After the incubation period, eGFP-CEM.NKr cells (NIH ARP-11698) were added as a reference population to calculate elimination of p24<sup>+</sup> or p24<sup>-</sup> 8E5 cells. Cells were stained with Aqua viability dye (ThermoFisher), then permeabilised with Cytofix/Cytoperm Fixation/Permeabilization Solution Kit (BD Biosciences) prior to staining with HIV p24 RD1 (KC57; Beckman Coulter, Mount Waverley, Australia). After intracellular staining, samples were washed and resuspended in PBS containing 2% FCS before acquisition on a BD LSR Fortessa using BD FACS Diva, with a consistent number of eGFP<sup>+</sup> CEM cells collected per tube. Percent cytotoxicity was calculated with the following formula:  $[(\%p24^+ \text{ compared to eGFP}^+ \text{ target alone} - \%p24^+ \text{ compared to eGFP}^+ \text{ experimental tube}) \div \%p24^+ \text{ compared to eGFP}^+ \text{ target alone}] \times 100$ .

### **Expression of ligands on target cells**

To assess the expression of ligands on the 8E5 cell line, cells were incubated with 5  $\mu$ g mL<sup>-1</sup> of NKG2D-Fc fusion protein (R&D Systems), 2B4-Fc fusion protein (R&D Systems), DNAM-1-Fc fusion protein (R&D Systems) or left unstained for 30 min, washed twice, then stained with Aqua viability dye (ThermoFisher). Binding of Fc-fusion proteins was detected with an APC-conjugated goat anti-human IgG antibody (HP6017; Biolegend). Samples were washed twice and then permeabilised with Cytofix/Cytoperm Fixation/Permeabilization Solution Kit (BD Biosciences) prior to staining with HIV p24 RD1 (KC57; Beckman Coulter). After intracellular staining, samples were washed and resuspended in PBS containing 2% FCS before acquisition on a BD LSR Fortessa using BD FACS Diva.

### **Flow cytometric phenotyping of *in vitro* expanded V $\delta$ 2 T cells**

On day 14 of expansion, V $\delta$ 2 T cells were collected and washed in PBS and stained with Aqua viability dye (ThermoFisher). Next, cells were surface stained for the following antibodies: CD26 FITC (BA5b, Biolegend), CD45RA PerCpCy5.5 (HI100; Biolegend), CD160 Alexa Fluor 647 (BY55; BD Biosciences), TIGIT APC Fire 750 (A15153G; Biolegend), PD-1 BV421 (EH12.2H7; Biolegend), NKG2D BV650 (1D11; BD Biosciences), CD27 BV786 (L128; BD Biosciences), CD94 BUV395 (HP-3D9; BD Biosciences), Tim-3 BUV737 (7D3; BD Biosciences), CD3 BUV805 (SK7; BD Biosciences), V $\delta$ 2 PE (B6; Biolegend) and 2B4 PE-Dazzle (C1.7; Biolegend). After surface staining, cells were washed and resuspended in PBS containing 2% FCS before acquisition on a BD LSR Fortessa using BD FACS Diva.

### **Statistics**

Flow cytometry data were analysed in FlowJo v10.2 (FlowJo, LLC, Ashland, USA). Statistical analyses were carried out using GraphPad Prism v10 (GraphPad, Boston, USA). Correlations were calculated using Spearman's *r*-test with two-tailed post-tests. Wilcoxon matched-pairs signed rank tests were performed for paired analysis. For unpaired data, Mann–Whitney *U*-tests were performed. For all *t*-tests, *P*-values < 0.05 were determined to be significant, otherwise ns.

## Study approval

The study was approved by the Alfred Health Human Research Ethics Committee (#337-12 and #432-14) and the University of Melbourne Human Ethics Review Committee (#11395).

## ACKNOWLEDGMENTS

We are grateful to both healthy volunteers and clinical subjects for their generous donation of samples for this study. We thank J Silvers, H Kent, A Kristensen, A Wheatley, M Parsons and the physicians at the Melbourne Sexual Health Centre for help recruiting subjects. We are grateful to C Batten, T Amarasena and J Rambhatla for technical assistance. We acknowledge the Melbourne Cytometry Platform for provision of flow cytometry services. The following reagents were obtained through the NIH HIV Reagent Program, Division of AIDS, NIAID, NIH: human immunodeficiency virus 1 (HIV-1) lymphadenopathy-associated virus (LAV)-infected 8E5 cells, ARP-95, contributed by Dr Thomas Folks; EGFP-CEMNR cells, ARP-11698, contributed by Dr Wannee Kantakamalaku; CEM.NKR CCR5<sup>+</sup> cells, ARP-4376, contributed by Dr Alexandra Trkola. JAJ, SJK and WSL are supported by NHMRC investigator grants and the project was funded by an NHMRC Program Grant (1149990). Open access publishing facilitated by The University of Melbourne, as part of the Wiley - The University of Melbourne agreement via the Council of Australian University Librarians.

## AUTHOR CONTRIBUTIONS

**Kirsty R Field:** Conceptualization; data curation; formal analysis; investigation; methodology; visualization; writing – original draft; writing – review and editing. **Kathleen M Wragg:** Data curation; investigation; writing – review and editing. **Stephen J Kent:** Funding acquisition; resources; writing – review and editing. **Wen Shi Lee:** Conceptualization; data curation; investigation; methodology; supervision; writing – review and editing. **Jennifer A Juno:** Conceptualization; funding acquisition; methodology; resources; supervision; writing – review and editing.

## CONFLICT OF INTEREST

The authors declare no conflict of interest.

## DATA AVAILABILITY STATEMENT

The data that support the findings of this study are available from the corresponding author upon request.

## REFERENCES

1. Perelson AS, Essunger P, Cao Y et al. Decay characteristics of HIV-1-infected compartments during combination therapy. *Nature* 1997; **387**: 188–191.

2. Palella FJ, Delaney KM, Moorman AC et al. Declining morbidity and mortality among patients with advanced human immunodeficiency virus infection. *N Engl J Med* 1998; **338**: 853–860.
3. Finzi D, Blankson J, Siliciano JD et al. Latent infection of CD4<sup>+</sup> T cells provides a mechanism for lifelong persistence of HIV-1, even in patients on effective combination therapy. *Nat Med* 1999; **5**: 512–517.
4. Siliciano JD, Kajdas J, Finzi D et al. Long-term follow-up studies confirm the stability of the latent reservoir for HIV-1 in resting CD4<sup>+</sup> T cells. *Nat Med* 2003; **9**: 727–728.
5. Fantoni M, Del Borgo C, Autore C. Evaluation and management of metabolic and coagulative disorders in HIV-infected patients receiving highly active antiretroviral therapy. *AIDS* 2003; **17**: S162–S169.
6. Gupta A, Wood R, Kaplan R, Bekker LG, Lawn SD. Tuberculosis incidence rates during 8 years of follow-up of an antiretroviral treatment cohort in South Africa: Comparison with rates in the community. *PLoS One* 2012; **7**: e34156.
7. Lawn SD, Bekker L-G, Wood R. How effectively does HAART restore immune responses to mycobacterium tuberculosis? Implications for tuberculosis control. *Aids* 2005; **19**: 1113–1124.
8. Macatangay BJC, Gandhi RT, Jones RB et al. T cells with high PD-1 expression are associated with lower HIV-specific immune responses despite long-term antiretroviral therapy. *Aids* 2020; **34**: 15–24.
9. Serrano-Villar S, Sainz T, Lee SA et al. HIV-infected individuals with low CD4/CD8 ratio despite effective antiretroviral therapy exhibit altered T cell subsets, heightened CD8<sup>+</sup> T cell activation, and increased risk of non-AIDS morbidity and mortality. *PLoS Pathog* 2014; **10**: e1004078.
10. Cockerham LR, Jain V, Sinclair E et al. Programmed death-1 expression on CD4<sup>+</sup> and CD8<sup>+</sup> T cells in treated and untreated HIV disease. *Aids* 2014; **28**: 1749–1758.
11. Jones RB, Ndhlovu LC, Barbour JD et al. Tim-3 expression defines a novel population of dysfunctional T cells with highly elevated frequencies in progressive HIV-1 infection. *J Exp Med* 2008; **205**: 2763–2779.
12. Sakhdari A, Mujib S, Vali B et al. Tim-3 negatively regulates cytotoxicity in exhausted CD8<sup>+</sup> T cells in HIV infection. *PLoS One* 2012; **7**: e40146.
13. Lundqvist C, Baranov V, Hammarström S, Athlin L, Hammarström ML. Intra-epithelial lymphocytes. Evidence for regional specialization and extrathymic T cell maturation in the human gut epithelium. *Int Immunol* 1995; **7**: 1473–1487.
14. Deusch K, Lüling F, Reich K, Classen M, Wagner H, Pfeffer K. A major fraction of human intraepithelial lymphocytes simultaneously expresses the  $\gamma\delta$  T cell receptor, the CD8 accessory molecule and preferentially uses the V $\delta$ 1 gene segment. *Eur J Immunol* 1991; **21**: 1053–1059.
15. Triebel F, Faure F, Graziani M, Jitsukawa S, Lefranc MP, Hercend T. A unique V-J-C-rearranged gene encodes a  $\gamma$  protein expressed on the majority of CD3<sup>+</sup> T cell receptor- $\alpha\beta$ - circulating lymphocytes. *J Exp Med* 1988; **167**: 694–699.
16. De Maria A, Ferrazin A, Ferrini S, Ciccone E, Terragna A, Moretta L. Selective increase of a subset of T cell receptor  $\gamma\delta$  T lymphocytes in the peripheral blood of patients with human immunodeficiency virus type 1 infection. *J Infect Dis* 1992; **165**: 917–919.

17. Li Z, Li W, Li N et al.  $\gamma\delta$  T cells are involved in acute HIV infection and associated with AIDS progression. *PLoS One* 2014; **9**: e106064.
18. Autran B, Triebel F, Katlama C, Rozenbaum W, Hercend T, Debre P. T cell receptor  $\gamma\delta^+$  lymphocyte subsets during HIV infection. *Clin Exp Immunol* 1989; **75**: 206–210.
19. Wesch D, Hinz T, Kabelitz D. Analysis of the TCR V $\gamma$  repertoire in healthy donors and HIV-1-infected individuals. *Int Immunol* 1998; **10**: 1067–1075.
20. Stankovic S, Davey MS, Shaw EM et al. Cytomegalovirus replication is associated with enrichment of distinct  $\gamma\delta$  T cell subsets following lung transplantation: A novel therapeutic approach? *J Heart Lung Transplant* 2020; **39**: 1300–1312.
21. Tuengel J, Ranchal S, Maslova A et al. Characterization of adaptive-like  $\gamma\delta$  T cells in Ugandan infants during primary cytomegalovirus infection. *Viruses* 2021; **13**: 1987.
22. Pitard V, Roumanes D, Lafarge X et al. Long-term expansion of effector/memory V $\delta 2^-$   $\gamma\delta$  T cells is a specific blood signature of CMV infection. *Blood* 2008; **112**: 1317–1324.
23. Halary F, Pitard V, Dlubek D et al. Shared reactivity of V $\delta 2^-$   $\gamma\delta$  T cells against cytomegalovirus-infected cells and tumor intestinal epithelial cells. *J Exp Med* 2005; **201**: 1567–1578.
24. Wallace M, Scharko AM, Pauza CD et al. Functional  $\gamma\delta$  T-lymphocyte defect associated with human immunodeficiency virus infections. *Mol Med* 1997; **3**: 60–71.
25. Bhatnagar N, Girard PM, Lopez-Gonzalez M et al. Potential role of V $\delta 2^+$   $\gamma\delta$  T cells in regulation of immune activation in primary HIV infection. *Front Immunol* 2017; **8**: 1189.
26. Martini F, Urso R, Gioia C et al.  $\gamma\delta$  T-cell anergy in human immunodeficiency virus-infected persons with opportunistic infections and recovery after highly active antiretroviral therapy. *Immunology* 2000; **100**: 481–486.
27. Casetti R, Sacchi A, Bordoni V et al. In human immunodeficiency virus primary infection, early combined antiretroviral therapy reduced  $\gamma\delta$  T-cell activation but failed to restore their polyfunctionality. *Immunology* 2019; **157**: 322–330.
28. Li H, Peng H, Ma P et al. Association between V $\gamma 2$ V $\delta 2$  T cells and disease progression after infection with closely related strains of HIV in China. *Clin Infect Dis* 2008; **46**: 1466–1472.
29. Poccia F, Boullier S, Lecoer H et al. Peripheral V $\gamma 9$ /V $\delta 2$  T cell deletion and anergy to nonpeptidic mycobacterial antigens in asymptomatic HIV-1-infected persons. *J Immunol* 1996; **157**: 449–461.
30. Kosub DA, Lehrman G, Milush JM et al. Gamma/Delta T-cell functional responses differ after pathogenic human immunodeficiency virus and nonpathogenic simian immunodeficiency virus infections. *J Virol* 2008; **82**: 1155–1165.
31. Dobmeyer TS, Dobmeyer R, Wesch D, Helm EB, Hoelzer D, Kabelitz D. Reciprocal alterations of Th1/Th2 function in  $\gamma\delta$  T-cell subsets of human immunodeficiency virus-1-infected patients. *Brit J Haematol* 2002; **118**: 282–288.
32. Bordon J, Evans PS, Propp N, Davis CE Jr, Redfield RR, Pauza CD. Association between longer duration of HIV-suppressive therapy and partial recovery of the V $\gamma 2$  T cell receptor repertoire. *J Infect Dis* 2004; **189**: 1482–1486.
33. Chaudhry S, Cairo C, Venturi V, Pauza CD. The  $\gamma\delta$  T-cell receptor repertoire is reconstituted in HIV patients after prolonged antiretroviral therapy. *Aids* 2013; **27**: 1557–1562.
34. Hebbeler AM, Propp N, Cairo C et al. Failure to restore the V $\gamma 2$ -J $\gamma 1.2$  repertoire in HIV-infected men receiving highly active antiretroviral therapy (HAART). *Clin Immunol* 2008; **128**: 349–357.
35. Li Z, Jiao Y, Hu Y et al. Distortion of memory V $\delta 2^-$   $\gamma\delta$  T cells contributes to immune dysfunction in chronic HIV infection. *Cell Mol Immunol* 2015; **12**: 604–614.
36. Pauza CD, Poonia B, Li H, Cairo C, Chaudhry S.  $\gamma\delta$  T cells in HIV disease: Past, present, and future. *Front Immunol* 2014; **5**: 687.
37. Casetti R, De Simone G, Sacchi A et al. V $\gamma 9$ V $\delta 2$  T-cell Polyfunctionality is differently modulated in HAART-treated HIV patients according to CD4 T-cell count. *PLoS One* 2015; **10**: e0132291.
38. Cummings JS, Cairo C, Armstrong C, Davis CE, Pauza CD. Impacts of HIV infection on V $\gamma 9$ V $\delta 2$  T cell phenotype and function: A mechanism for reduced tumor immunity in AIDS. *J Leukoc Biol* 2008; **84**: 371–379.
39. Boudová S, Li H, Sajadi MM, Redfield RR, Pauza CD. Impact of persistent HIV replication on CD4 negative V $\gamma 2$ V $\delta 2$  T cells. *J Infect Dis* 2012; **205**: 1448–1455.
40. Le Bouteiller P, Barakonyi A, Giustiniani J et al. Engagement of CD160 receptor by HLA-C is a triggering mechanism used by circulating natural killer (NK) cells to mediate cytotoxicity. *Proc Natl Acad Sci USA* 2002; **99**: 16963–16968.
41. Barakonyi A, Rabot M, Marie-Cardine A et al. Cutting edge: Engagement of CD160 by its HLA-C physiological ligand triggers a unique cytokine profile secretion in the cytotoxic peripheral blood NK cell subset. *J Immunol* 2004; **173**: 5349–5354.
42. Tu TC, Brown NK, Kim TJ et al. CD160 is essential for NK-mediated IFN- $\gamma$  production. *J Exp Med* 2015; **212**: 415–429.
43. Sun Z, Li Y, Zhang Z et al. CD160 promotes NK cell functions by upregulating glucose metabolism and negatively correlates with HIV disease progression. *Front Immunol* 2022; **13**: 854432.
44. Stanitsky N, Simic H, Arapovic J et al. The interaction of TIGIT with PVR and PVRL2 inhibits human NK cell cytotoxicity. *Proc Natl Acad Sci USA* 2009; **106**: 17858–17863.
45. Wang F, Hou H, Wu S et al. TIGIT expression levels on human NK cells correlate with functional heterogeneity among healthy individuals. *Eur J Immunol* 2015; **45**: 2886–2897.
46. Liu S, Zhang H, Li M et al. Recruitment of Grb2 and SHIP1 by the ITT-like motif of TIGIT suppresses granule polarization and cytotoxicity of NK cells. *Cell Death Differ* 2013; **20**: 456–464.
47. He Y, Peng H, Sun R et al. Contribution of inhibitory receptor TIGIT to NK cell education. *J Autoimmun* 2017; **81**: 1–12.
48. Vendrame E, Seiler C, Ranganath T et al. TIGIT is upregulated by HIV-1 infection and marks a highly functional adaptive and mature subset of natural killer cells. *Aids* 2020; **34**: 801–813.
49. Jia B, Zhao C, Claxton DF et al. TIGIT expression positively associates with NK cell function in AML patients. *Blood* 2018; **132**: 5250.

50. Ndhlovu LC, Lopez-Vergès S, Barbour JD et al. Tim-3 marks human natural killer cell maturation and suppresses cell-mediated cytotoxicity. *Blood* 2012; **119**: 3734–3743.
51. Golden-Mason L, Waasdorp Hurtado CE, Cheng L, Rosen HR. Hepatitis C viral infection is associated with activated cytolytic natural killer cells expressing high levels of T cell immunoglobulin- and mucin-domain-containing molecule-3. *Clin Immunol* 2015; **158**: 114–125.
52. Wang W, Erbe AK, Hank JA, Morris ZS, Sondel PM. NK cell-mediated antibody-dependent cellular cytotoxicity in cancer immunotherapy. *Front Immunol* 2015; **6**: 368.
53. So EC, Khaladj-Ghom A, Ji Y et al. NK cell expression of Tim-3: First impressions matter. *Immunobiology* 2019; **224**: 362–370.
54. Belkina AC, Starchenko A, Drake KA et al. Multivariate computational analysis of  $\gamma\delta$  T cell inhibitory receptor signatures reveals the divergence of healthy and ART-suppressed HIV+ aging. *Front Immunol* 2018; **9**: 2783.
55. Negash M, Tsegaye A, Wassie L, Howe R. Phenotypic and functional heterogeneity of peripheral  $\gamma\delta$  T cells in pulmonary TB and HIV patients in Addis Ababa, Ethiopia. *BMC Infect Dis* 2018; **18**: 464.
56. Wallace M, Bartz SR, Chang WL, Mackenzie DA, Pauza CD, Malkovsky M.  $\gamma\delta$  T lymphocyte responses to HIV. *Clin Exp Immunol* 1996; **103**: 177–184.
57. Garrido C, Clohosey ML, Whitworth CP, Hudgens M, Margolis DM, Soriano-Sarabia N.  $\gamma\delta$  T cells: An immunotherapeutic approach for HIV cure strategies. *JCI Insight* 2018; **3**: e120121.
58. Poccia F, Gioia C, Martini F et al. Zoledronic acid and interleukin-2 treatment improves immunocompetence in HIV-infected persons by activating V $\gamma$ 9V $\delta$ 2 T cells. *AIDS* 2009; **23**: 555–565.
59. James KS, Trumble I, Clohosey ML et al. Measuring the contribution of  $\gamma\delta$  T cells to the persistent HIV reservoir. *Aids* 2020; **34**: 363–371.
60. Kobayashi H, Tanaka Y.  $\gamma\delta$  T cell immunotherapy-a review. *Pharmaceuticals (Basel)* 2015; **8**: 40–61.
61. Hoeres T, Smetak M, Pretscher D, Wilhelm M. Improving the efficiency of V $\gamma$ 9V $\delta$ 2 T-cell immunotherapy in cancer. *Front Immunol* 2018; **9**: 800.
62. Fisher JP, Heuveljans J, Yan M, Gustafsson K, Anderson J.  $\gamma\delta$  T cells for cancer immunotherapy: A systematic review of clinical trials. *Oncoimmunology* 2014; **3**: e27572.
63. Lo Presti E, Pizzolato G, Gulotta E et al. Current advances in  $\gamma\delta$  T cell-based tumor immunotherapy. *Front Immunol* 2017; **8**: 1401.
64. Almeida AR, Correia DV, Fernandes-Platzgummer A et al. Delta one T cells for immunotherapy of chronic lymphocytic leukemia: Clinical-grade expansion/differentiation and preclinical proof of concept. *Clin Cancer Res* 2016; **22**: 5795–5804.
65. Couzi L, Pitard V, Sicard X et al. Antibody-dependent anti-cytomegalovirus activity of human  $\gamma\delta$  T cells expressing CD16 (Fc $\gamma$ R11a). *Blood* 2012; **119**: 1418–1427.
66. Bachelet T, Couzi L, Pitard V et al. Cytomegalovirus-responsive  $\gamma\delta$  T cells: Novel effector cells in antibody-mediated kidney allograft microcirculation lesions. *J Am Soc Nephrol* 2014; **25**: 2471–2482.
67. de Witte MA, Sarhan D, Davis Z et al. Early reconstitution of NK and  $\gamma\delta$  T cells and its implication for the design of post-transplant immunotherapy. *Biol Blood Marrow Transplant* 2018; **24**: 1152–1162.
68. Bruel T, Guivel-Benhassine F, Amraoui S et al. Elimination of HIV-1-infected cells by broadly neutralizing antibodies. *Nat Commun* 2016; **7**: 10844.
69. Fausther-Bovendo H, Wauquier N, Cherfils-Vicini J, Cremer I, Debré P, Vieillard V. NKG2C is a major triggering receptor involved in the V $\delta$ 1 T cell-mediated cytotoxicity against HIV-infected CD4 T cells. *AIDS* 2008; **22**: 217–226.
70. Poles MA, Barsoum S, Yu W et al. Human immunodeficiency virus type 1 induces persistent changes in mucosal and blood  $\gamma\delta$  T cells despite suppressive therapy. *J Virol* 2003; **77**: 10456–10467.
71. Kristensen AB, Wragg KM, Vandervan HA et al. Phenotypic and functional characteristics of highly differentiated CD57<sup>+</sup>NKG2C<sup>+</sup> NK cells in HIV-1-infected individuals. *Clin Exp Immunol* 2022; **210**: 163–174.
72. Gleason MK, Lenvik TR, McCullar V et al. Tim-3 is an inducible human natural killer cell receptor that enhances interferon gamma production in response to galectin-9. *Blood* 2012; **119**: 3064–3072.
73. Kondo M, Sakuta K, Noguchi A et al. Zoledronate facilitates large-scale ex vivo expansion of functional  $\gamma\delta$  T cells from cancer patients for use in adoptive immunotherapy. *Cytotherapy* 2008; **10**: 842–856.
74. Lee WS, Kristensen AB, Rasmussen TA et al. Anti-HIV-1 ADCC antibodies following latency reversal and treatment interruption. *J Virol* 2017; **91**: e00603–e00617.
75. Folks TM, Powell D, Lightfoote M et al. Biological and biochemical characterization of a cloned Leu-3- cell surviving infection with the acquired immune deficiency syndrome retrovirus. *J Exp Med* 1986; **164**: 280–290.
76. Wilburn KM, Mwandumba HC, Jambo KC et al. Heterogeneous loss of HIV transcription and proviral DNA from 8E5/LAV lymphoblastic leukemia cells revealed by RNA FISH: FLOW analyses. *Retrovirology* 2016; **13**: 55.
77. Lerner AM, Eisinger RW, Fauci AS. Comorbidities in persons with HIV: The lingering challenge. *JAMA* 2020; **323**: 19–20.
78. Sharan R, Bucşan AN, Ganatra S et al. Chronic immune activation in TB/HIV co-infection. *Trends Microbiol* 2020; **28**: 619–632.
79. Brenchley JM, Price DA, Schacker TW et al. Microbial translocation is a cause of systemic immune activation in chronic HIV infection. *Nat Med* 2006; **12**: 1365–1371.
80. Guadalupe M, Reay E, Sankaran S et al. Severe CD4<sup>+</sup> T-cell depletion in gut lymphoid tissue during primary human immunodeficiency virus type 1 infection and substantial delay in restoration following highly active antiretroviral therapy. *J Virol* 2003; **77**: 11708–11717.
81. Dillon SM, Frank DN, Wilson CC. The gut microbiome and HIV-1 pathogenesis: A two-way street. *Aids* 2016; **30**: 2737–2751.
82. Olson GS, Moore SW, Richter JM et al. Increased frequency of systemic pro-inflammatory V $\delta$ 1<sup>+</sup>  $\gamma\delta$  T cells in HIV elite controllers correlates with gut viral load. *Sci Rep* 2018; **8**: 16471.
83. Boullier S, Dadaglio G, Lefeuvre A, Debord T, Gougeon ML. V $\delta$ 1 T cells expanded in the blood throughout HIV infection display a cytotoxic activity and are primed for TNF- $\alpha$  and IFN- $\gamma$  production but are not selected in lymph nodes. *J Immunol* 1997; **159**: 3629–3637.
84. Fenoglio D, Poggi A, Catellani S et al. V $\delta$ 1 T lymphocytes producing IFN- $\gamma$  and IL-17 are expanded in HIV-1-infected patients and respond to *Candida albicans*. *Blood* 2009; **113**: 6611–6618.



85. Chevalier MF, Bhatnagar N, Didier C *et al.*  $\gamma\delta$  T-cell subsets in HIV controllers: Potential role of  $\gamma\delta 17$  cells in the regulation of chronic immune activation. *AIDS* 2019; **33**: 1283–1292.
86. Cimini E, Agrati C, D'Offizi G *et al.* Primary and chronic HIV infection differently modulates mucosal  $V\delta 1$  and  $V\delta 2$  T-cells differentiation profile and effector functions. *PLoS One* 2015; **10**: e0129771.
87. Rossol R, Dobmeyer JM, Dobmeyer TS *et al.* Increase in  $V\delta 1^+\gamma\delta$  T cells in the peripheral blood and bone marrow as a selective feature of HIV-1 but not other virus infections. *Br J Haematol* 1998; **100**: 728–734.
88. Hatano H, Somsouk M, Sinclair E *et al.* Comparison of HIV DNA and RNA in gut-associated lymphoid tissue of HIV-infected controllers and noncontrollers. *Aids* 2013; **27**: 2255–2260.
89. Gianella S, Letendre S. Cytomegalovirus and HIV: A dangerous pas de deux. *J Infect Dis* 2016; **214 Suppl 2**: S67–S74.
90. Gianella S, Massanella M, Wertheim JO, Smith DM. The sordid affair between human herpesvirus and HIV. *J Infect Dis* 2015; **212**: 845–852.
91. Vujkovic-Cvijin I, Somsouk M. HIV and the gut microbiota: Composition, consequences, and avenues for amelioration. *Curr HIV/AIDS Rep* 2019; **16**: 204–213.
92. Sindhu ST, Ahmad R, Morisset R, Ahmad A, Menezes J. Peripheral blood cytotoxic  $\gamma\delta$  T lymphocytes from patients with human immunodeficiency virus type 1 infection and AIDS lyse uninfected  $CD4^+$  T cells, and their cytotoxic potential correlates with viral load. *J Virol* 2003; **77**: 1848–1855.
93. Sacchi A, Rinaldi A, Tumino N *et al.* HIV infection of monocytes-derived dendritic cells inhibits  $V\gamma 9V\delta 2$  T cells functions. *PLoS One* 2014; **9**: e111095.
94. Cardone M, Ikeda KN, Varano B, Gessani S, Conti L. HIV-1-induced impairment of dendritic cell cross talk with  $\gamma\delta$  T lymphocytes. *J Virol* 2015; **89**: 4798–4808.
95. Rigau M, Ostrouska S, Fulford TS *et al.* Butyrophilin 2A1 is essential for phosphoantigen reactivity by  $\gamma\delta$  T cells. *Science* 2020; **367**: eaay5516.
96. Harly C, Guillaume Y, Nedellec S *et al.* Key implication of CD277/butyrophilin-3 (BTN3A) in cellular stress sensing by a major human  $\gamma\delta$  T-cell subset. *Blood* 2012; **120**: 2269–2279.
97. Ward J, Bonaparte M, Sacks J *et al.* HIV modulates the expression of ligands important in triggering natural killer cell cytotoxic responses on infected primary T-cell blasts. *Blood* 2007; **110**: 1207–1214.

## Supporting Information

Additional supporting information may be found online in the Supporting Information section at the end of the article.



This is an open access article under the terms of the [Creative Commons Attribution](#) License, which permits use, distribution and reproduction in any medium, provided the original work is properly cited.